(Received 15 February 2024, Accepted 19 May 2024, Scheduled 3 June 2024)

Control Signals for NOMA-VLC Systems

Safwan Hafeedh Younus* and Mohamad A. Ahmed

College of Electronics Engineering, Ninevah University, Mosul, P. O. 41002, Iraq

ABSTRACT: In wireless communication systems, a control signal (CS) plays a vital role in managing the connection between transmitters (Txs) and the user equipment (UEs). This work presents CSs for non-orthogonal multiple access (NOMA)-based on visible light communication (VLC) systems. Moreover, pairing schemes, successive interference cancellation (SIC), and load balancing are considered with the NOMA-VLC technique for enhancing the entire performance. The CSs, which are single tones or can be described as unmodulated signals, are exploited to estimate the channel between Txs and UEs, and to evaluate the amount of interference at each UE. Thus, a controller, which is employed to manage the connections between Txs and UEs, can balance the load between Txs based on the level of interference at each UE. Each Tx is allocated a unique CS, i.e., a single-tone frequency. A power measurement unit (PMU) is utilized at each UE for measuring the power of each CS. Therefore, the controller divides the UEs into small groups based on the feedback signals from the PMU, then each group is connected to one Tx. Besides, CSs are used to find the optimum number of UEs that can be served by each Tx with a particular data rate of 50 Mbps and with an acceptable error probability of 10^{-6}, by utilizing on-off keying (OOK) modulation scheme.

1. INTRODUCTION

In visible light communication (VLC) systems, numerous transmitters (Txs) with small coverage areas can be employed to attain illumination at an acceptable level. For wireless communication, Txs with small coverage areas increase the capacity of wireless systems and reduce path losses. However, supporting multi-users simultaneously may add more complexity related to signal processing and managing the transmission. Thus, a suitable multiple access scheme is required especially when the area between the Txs is limited. In this context, non-orthogonal multiple access (NOMA) is proposed for indoor multiple access of visible light communication (VLC) systems [1, 2]. NOMA is one of the promising multiplexing mechanisms for the next generation of wireless communications. This technique has witnessed lots of interest due to its ability to enhance the spectral efficiency significantly compared to the conventional orthogonal multiplexing access (OMA). NOMA can also provide massive connectivity and satisfy user fairness for future wireless communications. By utilizing this multiplexing method, the signals of multiple users are superposed in the power domain (PD) at the transmitter, while demultiplexing is achieved at each user equipment (UE) to detect its signal. In a wireless system that uses optical communication, power allocation factors (PAFs) are provided to each UE before multiplexing in the power domain, in which the UEs with weak channel circumstances are allocated higher portions of the available transmitter power. Successive interference cancellation (SIC) is required for disassembling the multiplexed signals. It is noteworthy that the highest order UE, i.e., the UE that allocated highest PAF, does not need SIC at its optical receiver by considering the other superposed signal as just an additive noise [1, 3]. In the literature on visible optical wireless communication with NOMA, the latter has been used with reconfigurable intelligent surfaces (RISs) to improve the capacity of VLC systems [4]. The angle diversity receiver is investigated for VLC in [5] for the sake of obtaining higher throughput, in which an enhancement of 35% of the data rate is achieved compared to VLC systems that use traditional wide field of view (FOV) detectors. In [6], the cooperative power domain NOMA is suggested for downlink VLC, where the achievable rates and error probabilities are derived in the presence of cooperative and noncooperative PD-NOMA by assuming the availability of perfect channel state information (CSI). In [7], NOMA is proposed for indoor VLC and compared with conventional orthogonal frequency division multiple access (OFDMA). The proposed system of NOMA-VLC outperforms the OFDMA system under the same condition, with considerable complexity of the receiving circuit noticed for VLC. In these contexts, the main strategies of PAF and pairing algorithms are introduced in [8] for NOMA-based VLC systems, in which different performance metrics are taken into account between these strategies and algorithms. In the literature, CSs have been used as adaptation methods to reduce the amount of interference at each UE [9]. In [10], CSs have been proposed with a differential receiver to enhance the performance of the wavelength division multiplexing (WDM) based on VLC systems. Additionally, CSs have been proposed and applied for handover mechanisms in indoor VLC systems [11]. The amount of crosstalk that has been noticed by each channel of dense WDM optical wireless communication systems was reduced significantly by using the CSs [11]. The main contribution of this work can be summarized as the proposal of CSs to measure the channel circumstance of each link between all Txs and UEs, in which

* Corresponding author: Safwan afeedh Younus (safwan.younus@uoninevah.edu.iq).

the states of these channels are used for coupling a group of UEs with a Tx via applying a pairing algorithm. Furthermore, mechanisms, such as SIC and load balancing, are utilized with NOMA-VLC systems for managing the interference and enhancing the overall performance. To the best of our knowledge, this is the first time that CSs are employed with NOMA-VLC systems for this purpose, in which each Tx is allocated a unique CS, i.e., single tone or can be named unmodulated signal. These single-tone signals can be used in VLC systems for numerous purposes. Here, CSs are proposed to i) identify each Tx, ii) estimate the channel between each Tx and its related UEs, and iii) find the amount of interference that can be noticed by each UE. The total output power from each Tx is divided between the data signal and the CS. Besides, at each UE, a power measurement unit (PMU) is used to measure the amount of the received power of each CS. Therefore, the channel between any UE and a Tx is required to be estimated accurately to achieve this mission. Consequently, UEs are divided into many small groups, and each group is related to one Tx. Moreover, by measuring the received power of a CS at each UE, the amount of interference can be estimated, and the SIC can be enabled to extract the desired power of each UE. Besides that, CSs are proposed to distribute the load between Txs to attain the required data rates with high link performance.

The paper is organized as follows. Section 2 describes the proposed VLC system. Section 3 presents and discusses simulation results. Finally, Section 4 closes the paper with some conclusions.

2. SYSTEM DESCRIPTION

In this work, an empty room that has a dimension of 6 m × 6 m × 3 m (length × width × height) with no furniture, doors, or windows is proposed to model our system. The system comprises four Txs that are located at (2 m, 2 m, 3 m), (2 m, 4 m, 3 m), (4 m, 2 m, 3 m), and (4 m, 4 m, 3 m) as shown in Fig. 1. To modal the indoor channel, we use the ray tracing algorithm similar to the one in [12–14]. Each Tx has 16 light diodes (LDs), i.e., (4 × 4), and the output power of each LD is 1.9 W [15]. Moreover, the distance between LDs in a Tx is 0.1 cm. Two

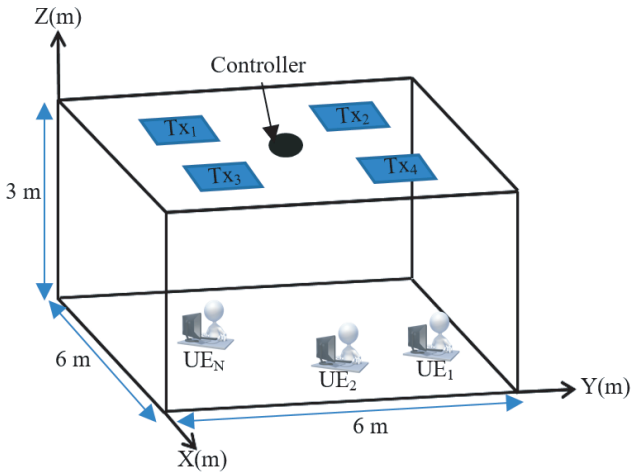

FIGURE 1. Room construction.

signals are transmitted from each Tx, which are the data signal and CS. To calculate the power of each CS at a particular UE, each single UE is equipped with some band-pass filters (BPFs) that equal the number of the Txs (here, each UE has four BPFs). Furthermore, each BPF has a center frequency that is equal to the frequency of each CS in a Tx. A PMU is employed in each UE to capture the output of each BPF and calculate the power of the CSs in each UE as depicted in Fig. 2. A low pass filter (LPF) is also utilized in each UE to capture the data signal as shown in Fig. 2.

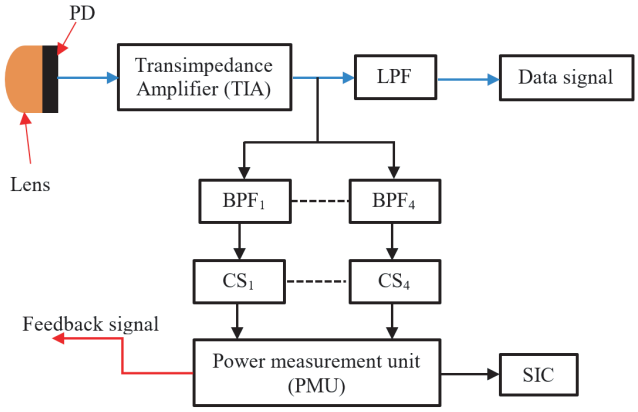

FIGURE 2. UE's receiver configuration.

Each Tx is given a unique CS, which is used for estimating the channels. Each UE has several BPFs with center frequencies equal to the frequency of the CS in each Tx. The total input current, I_{Tx}, at each Tx can be expressed as:

$$I_{Tx} = k_1 I_{DS} + k_2 I_{CS}, \tag{1}$$

where I_{DS} denotes the current of the data signal, and I_{CS} is the current of the CS. Additionally, k_1 and k_2 are the power coefficient factors of the data signal and the CS in each Tx, respectively, with $(k_1 + k_2 = 1)$. Therefore, the total output optical power from each Tx, P_{Tx}, is divided between the information signal and CS, and it is given as:

$$P_{Tx} = k_1 P_{Tx} + k_2 P_{Tx}, \tag{2}$$

It is noteworthy that the CS is a cosine signal that can be generated by using a local oscillator, and it is given as $CS(t) = A\cos(wt)$, where A is the peak amplitude of the CS, and w is the radian frequency of the control signal $(w = 2\pi f)$. We emphasize that each Tx is given a unique frequency. The parameters that are used in this work are summarized in Table 1.

2.1. Control Signals for Pairing Schemes

As mentioned earlier in this section, each Tx is equipped with a unique CS that is employed to estimate the channel between any UE and the available Txs. At each UE, a PMU is installed to estimate the power of each CS, as shown in Fig. 2. The electrical output power from the k_{th} BPF at the n_{th} UE, $P_{CS_{kn}}$ can be given as:

$$P_{CS_{kn}} = \frac{(Rk_2 P_{Tx} h_{kn})^2}{2}, \tag{3}$$

TABLE 1. System parameters.

Parameters	Values
Room size (length, width, height)	6 m × 6 m × 3 m
Reflection constant of walls	0.8 [16]
Emission order of the walls	1 [16]
Number of Txs	4
Number of LDs/Txs	16 (4 × 4)
The optical power of each LD	1.9 W [15]
LD center luminous intensity	162 cd [15]
LD half-power semi-angle	60°
Field of view of the photodiode	90°
Photodiode's area	5 mm^2
Photodiode's responsivity	0.4 A/W [17]
Receiver's bandwidth	0.6 GHz [18]
Thermal noise current density	4.5 pA/$\sqrt{\text{Hz}}$ [19]
Ambient noise photocurrent	10^{-3} A/cm^2 [20]
Locations of Txs	(2 m, 2 m, 3 m)
	(2 m, 4 m, 3 m)
	(4 m, 2 m, 3 m)
	(4 m, 4 m, 3 m)

where h_{kn} denotes the channel gain between k_{th} Tx and n_{th} UE, while R represents the responsivity of the photodiode. It is worth noting that we consider scenarios that include transmission of signal with line-of-sight (LoS) and non-LoS (NLOS) components (up to 3rd-order reflections) to find h_{kn} and to evaluate h_{kn} similar to [13, 14]. Consequently, the carrier-to-noise ratio (CNR) of each CS at each UE, which can be denoted as $\Upsilon_{CS_{kn}}$, can be expressed as:

$$\Upsilon_{CS_{kn}} = \frac{P_{CS_{kn}}}{\sigma_{CS}^2} = \frac{(Rk_2P_{Tx}h_{kn})^2}{2\left(\sigma_{CS_{th}}^2 + \sigma_{CS_{bn}}^2\right)}, \tag{4}$$

where σ_{CS} is the total noise measured by the CS, while $\sigma_{CS_{th}}$ is the thermal noise of the pre-amplifier, and $\sigma_{CS_{bn}}$ is the background noise, which can be calculated as in [20]. Therefore, the **H** matrix is formed by the $\Upsilon_{CS_{kn}}$ as:

$$\mathbf{H} = \begin{bmatrix} \Upsilon_{CS_{11}} & \cdots & \Upsilon_{CS_{1N}} \\ \vdots & \cdots & \vdots \\ \Upsilon_{CS_{k41n}} & \cdots & \Upsilon_{CS_{4N}} \end{bmatrix}. \tag{5}$$

Furthermore, a feedback signal is sent from the PMU to the controller to inform the latter of all the measured values of the elements of **H**, i.e., $\Upsilon_{CS_{kn}}$, that are measured at each UE for the transmitted signal from each Tx.

Hence, the controller acquires information about the channel between Txs and UEs. Based on the values of the elements in the **H** matrix at each UE, the controller divides the UEs into four groups, as there are four Txs in our proposed room, and each group is associated with one Tx. Additionally, the controller sorts the UEs in ascending order in each group based on their level of CNR. It is noteworthy that in some locations UEs may receive the same CNR from two or more Txs. In this case, the controller assigns one Tx to this UE based on the number of UEs in each Tx (load balancing) as will be explained and discussed later. Once the controller divides the UEs into groups, each UE is paired with its corresponding UE in the same group. Several pairing algorithms can be used in NOMA-VLC systems. In this work, we assume the pairing algorithm that has been proposed in [21] due to its simplicity, and in this work, we are focusing in CSs in NOMA transmission.

2.2. Control Signals for SIC

In NOMA, SIC plays a significant role in reducing the amount of interference at the UEs to an acceptable level. This technique decodes the signal of the strong user, then subtract it from the entire NOMA signal to detect the weak user's signal. As each UE is given a specific portion of the total power of the Tx (the closest UE to the Tx is given a lower power than the furthest UE to the Tx), the SIC should be operated at the closest UE to detect its signal. For a scenario that assumes two UEs, the SIC is used only at the closest UE to eliminate the signal of the furthest UE, which is considered an interference signal at this user terminal. The first phase of SIC is started by detecting the signal of the furthest UE, i.e., the UE which has been allocated more portion of the available power. In the second phase, the detected signal of the furthest UE is subtracted from the entire received NOMA signal at the next order UE, i.e., the UE with the lower portion of the power next to the furthest UE. After this subtraction process is accomplished, the signal can be detected by the UE of interest after removing the interference caused by the superposed NOMA signal. It is noteworthy that this process is repeated at each UE's terminal, except the furthest UE, by removing the interfered signal of the higher order UE and considering the signal of the lower signal UE as just an additive noise. Once the electrical received power of each CS is measured at each UE by PMU, the PMU sends a feedback signal to the SIC block (see Fig. 2), which enables the controller to measure the level of interference at the nearest UE. However, the PMU is used to calculate the power of each CS from each Tx. Thus, it is very important to find the power of the data signals from the CS. The electrical power of the data signal at any UE due to any Tx, $P_{DS_{kn}}$, is given as:

$$P_{DS_{kn}} = \left[R(1-k_2)P_{Tx}h_{kn}\right]^2, \tag{6}$$

Dividing (6) by (3) the electrical power of the data can be related to the electrical power of the CS as:

$$P_{DS_{kn}} = 2\left(\frac{1-k_2}{k_2}\right)^2 P_{CS_{kn}}. \tag{7}$$

Thus, the amount of assigned power for each UE in each group will be known at the SIC block in each UE. This enables the SIC to estimate the total interference at each UE correctly. The total interference at any UE from its associated Tx, I_{T_S}, can be given as:

$$I_{T_S}(k) = \sum_{n=1}^{S-1} P_{DS_{kn}} = 2\left(\frac{1-k_2}{k_2}\right)^2 \sum_{n=1}^{S-1} P_{CS_{kn}}, \tag{8}$$

where the subscript S refers to the number of UEs in each group. It is worth knowing that each Tx is used to serve its associated

group. In addition, the pairing algorithm is applied to reduce the complexity of the system, so we can deal with small groups of two UEs. However, we take into account the effect of all interference from all UEs in the same Tx. It should be noted that due to using NOMA, each UE is given a level of power in the power domain. It means that the signal of each UE appears as interference to other UE.

2.3. Control Signals for Load Balancing

As mentioned earlier, UEs are divided into four groups (as we have four Txs), and each group is served by its associated Tx. In addition, the controller ascends in order the UEs in each group based on the channel estimation from the CSs. Hence, each UE in each group is assigned a part of the total power of its associated Tx (the closest UE is given the lowest power, while the furthest one is given the highest power). The performance of each UE is estimated by the signal-to-interference-plus-noise ratio (SINR) or the signal-to-noise ratio (SNR) depending on whether it needs to apply SIC or not, respectively. If the assigned power of $UE_S > UE_{S-1} > \ldots > UE1$, UE1 is the closest one to its Tx. The SNR for the S_{th} user is given as:

$$SNR_S = \frac{2\left(\frac{1-k_2}{k_2}\right)^2 P_{CS_S}}{\sigma^2_{DS_S}}, \tag{9}$$

while the SINR of the i_{th} user can be expressed as

$$SINR_i = \frac{2\left(\frac{1-k_2}{k_2}\right)^2 P_{CS_i}}{\sum_{l=1,l\neq i}^{S-1} 2\left(\frac{1-k_2}{k_2}\right)^2 P_{CS_l} + \sigma^2_{DS_S}}, \tag{10}$$

where σ_{DS} is the standard deviation of the total noise that affects the data signal. In this work, we consider two types of noises, thermal noise and background noise. For the thermal noise, we assumed the receiver that has been presented in [19] which has a noise current of $(4.5\,\text{pA})/\sqrt{\text{Hz}}$. It is worth knowing that to find σ_{DS}, we consider the receiver bandwidth, while to find σ_{CS} we used the BPFs' bandwidth. Consequently, the total achievable throughput (R_T) of each Tx can be given as:

$$R_T = BW_{DS}\left(\sum_{i=1}^{S-1} \log_2(1+SINR_i)+\log_2(1+SNR_i)\right), \tag{11}$$

where BW_{DS} is the bandwidth of the data signal.

In this work, the OOK scheme is used. Thus, the bit error rate (BER) of each UE can be calculated as:

$$BER_S = Q\left(\frac{2\left(\frac{1-k_2}{k_2}\right)^2 P_{CS_S}}{\sigma^2_{DS_S}}\right), \tag{12}$$

$$BER_i = Q\left(\frac{2\left(\frac{1-k_2}{k_2}\right)^2 P_{CS_i}}{\sum_{l=1,l\neq i}^{S-1} 2\left(\frac{1-k_2}{k_2}\right)^2 P_{CS_l} + \sigma^2_{DS_S}}\right) \tag{13}$$

where $Q(z) = \frac{1}{\sqrt{2\pi}}\int_z^\infty e^{(\frac{-y^2}{2})}dy$ represents the Q-function. In this work, we assume that each UE is served with no more than 10^{-6} of an acceptable BER. Thus, the controller observes the performance of each UE in a particular group, and if any UE has a BER worse than 10^{-6}, the controller changes the Tx of this UE. This process can be achieved due to the large coverage area of the proposed Tx that can serve any UE in this room. In more detail, the semi-angle of each Tx was 60°, which makes each Tx cover an area with a radius equal to $2 \times \tan(60°)$ as the communication floor of the UE is assumed equal to 1 m. Consequently, the overlap area between Txs is high as shown in Fig. 3. It should be noted that the overlap area between Txs is designed to be large enough to attain an acceptable lighting level in the proposed room. Hence, if any UE is positioned in the overlapping area between Txs, the controller can move it to any Tx that has a few UEs to achieve load balancing between Txs.

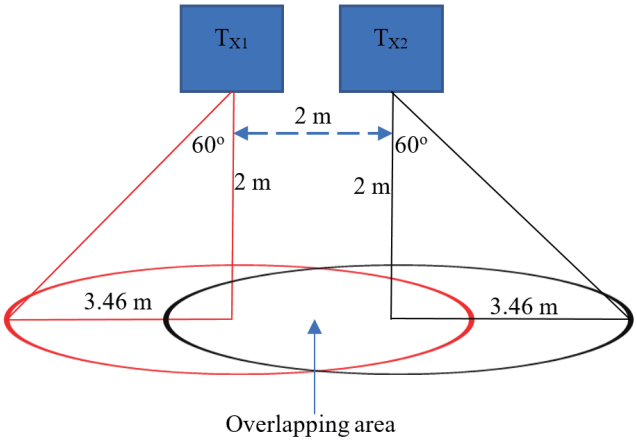

FIGURE 3. Coverage area of each Tx.

3. SIMULATION RESULTS AND DISCUSSION

In this paper, the total bandwidth (BW) of the system is split between data signals and CSs. It should be noticed that the BW of the VLC systems can be limited by the BW of Tx, the BW of UE, or the BW of the channel. However, an LD is used in this work, which has a high BW. In addition, the size of the photodiode is selected to be 5 mm^2, which enables the photodiode to work at BW up to 0.61 GHz. Relationships between the area of the photodiode and its BW can be found in [18]. Therefore, we consider that the channel BW is the system's BW in this work. This is due to the BW of the channel having a lower value than the BW of the LD and the BW of the photodiode. Fig. 4 depicts the channel BW of a UE while this UE was located at the room corner (0.5 m, 0.5 m, 1 m) and related to Tx1. This location was selected as the UE suffers from high multipath (worst-case scenario), which leads to reducing the channel BW. It should be noted that to obtain the channel BW of our proposed system, the impulse response is obtained by utilizing the approach used in [14]. At each location of the UE, we obtain the impulse response and then find the channel BW. As can be seen from Fig. 4, the channel BW of this UE is 150 MHz. Thus, we consider this BW to be the system's BW. The total BW of the indoor

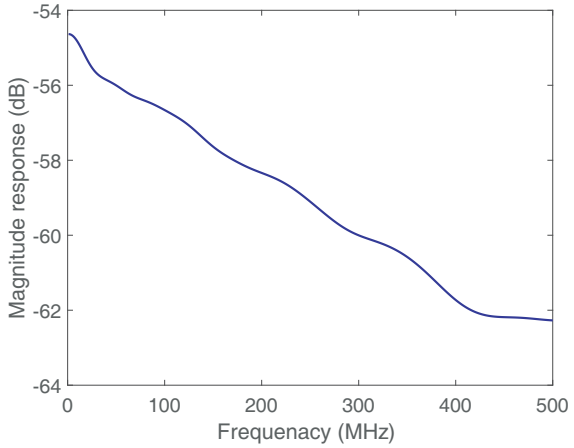

FIGURE 4. Frequency response of the UE that was located at the room corner (0.5 m, 0.5 m, 1 m) and connected with Tx1.

VLC system is divided between data signals, BW_{DS}, and CSs (BW_{CS}). In this work, BW_{DS} is assumed to be 100 MHz. In addition, BW_{CS} is selected to be 8 MHz, which was assumed to be equal to the BW of BPFs. The first CS (CS of Tx1) is given a frequency of 110 MHz while the last CS (CS of Tx4) is given a frequency of 140 MHz. It means that the guard band between CSs is assumed equal to 10 MHz, which reduces the interference between the CSs. As explained earlier, the total output power of each Tx is divided between data signals and CS. In addition, the total BW of the indoor VLC systems is split between the data signal and CS in each Tx. Thus, calculating the amount of allocated power and the amount of the BW of each CS is very important in our proposed system. As the probability of error in the channel estimation of the CS depends on the power coefficient factor (k_2), increasing the value of k_2 leads to a decrease in the amount of power that is allocated to data signals, consequently, reducing the data rate of UEs. The probability of error of any CS, Pe_{CS}, can be given as:

$$Pe_{CS} = \frac{1}{2} erfc\left(\frac{\Upsilon_{CS}}{\sqrt{2}}\right) = \frac{1}{2} erfc\left(\frac{(Rk_2 P_{Tx} h_{kn})^2}{2\sqrt{2}(\sigma^2_{CS_{th}} + \sigma^2_{CS_{bn}})}\right), \quad (14)$$

where $erfc(\cdot)$ denotes the error function complementary. We emphasize that the probability of error of the CS means the error in the decision of the controller to allocate each UE its best Tx.

Figure 5 shows the effect k_2 of on Pe_{CS} when a UE is located at the corner of the room (0.5 m, 0.5 m, 1 m), and it is assumed to be connected to Tx1. As can be seen, increasing the value of k_2 leads to reducing the Pe_{CS}. However, we assume that each UE is served with BER not more than 10^{-6}. Therefore, we consider that the Pe_{CS} is not more than 10^{-6}. This can be achieved when k_2 is equal to 0.3 approximately, i.e., each CS in each Tx is given 30% of the transmitted power. It is worth knowing that we use the BW of the BPF to calculate the $\sigma_{CS_{th}}$.

Due to the symmetry of our proposed room, we obtained the result of one Tx, which is Tx1. In addition, we assume that Txs are separated in frequencies. Thus, the interference between Txs is ignored in this work. In addition, we assume that the UEs are distributed randomly on the communication floor of Tx1. It should be noted that the minimum space between UEs is 0.3 m [22], and there are no two UEs, or users with multiple equipment, are located at the same place as assumed in this work. In this work, we selected the distance to be 0.3 m, which represents a realistic distance. Normally, the minimum distance between two persons is about 0.3 m. In this paper, we assume that each UE is served with BER not more than 10^{-6}. Besides, in each group, the interference is high at the closest UE to its Tx. Thus, the number of UEs that can be served by each Tx with the accepted BER is evaluated as shown in Fig. 6. In this figure, the SINRs of the closest UE to Tx1 versus the number of UEs are shown over different horizontal distances. The results are obtained by distributing UEs randomly on the communication floor of the coverage area of the Tx1 with a data rate of 50 Mbps for each UE. Furthermore, we consider different horizontal distances between the closest UE and Tx1, which are 0 m, 0.25 m, and 0.5 m. Moreover, all UEs are distributed randomly further than the closest UE from the Tx1. It should be noted that other UEs are randomly distributed while considering the distance between UEs not less than 0.3 m. As can be noticed in Fig. 6, increasing the number of UEs causes degradation of the SINR since the allocated power to the closest UE and the amount of interference at this UE are changed when the number of UEs is increased based on the feedback signal from the PMU. For example, when we have two UEs, the controller assigns the required power to each UE to obtain a data rate of 50 Mbps with less than 10^{-6} BER, which means that each UE is assigned only the amount of the required power to meet the required data rate with this BER, and this is based on the feedback signal from the PMU. As shown in Fig. 6, the best performance is when the distance between the closest UE and Tx1 is equal to 0 m. This is because all UEs are close to Tx1, which means that the attenuation at these distances is low. However, when the closest UE is at 0.5 m from Tx1, the maximum number of UEs, which can be served with a data rate of 50 Mbps and the assumed acceptable BER, is 5 UEs with OOK modulation schemes, where the SINR should be 13.6 dB. Thus, we can conclude that our proposed system can serve around 20 UEs with the above specifications.

Figure 7 depicts the total throughput of Tx1 with the number of UEs. The results are obtained when distributing UEs randomly in the coverage area of Tx1. Moreover, each UE is served with the assumed acceptable BER and with SINR equal to or above 13.6 dB. As can be noticed from Fig. 7, increasing the number of UEs leads to enhancing the throughput of Tx1. It should be noted that each UE is served with a data rate of 50 Mbps when the number of UEs is up to 5 with the mentioned BER. However, by increasing the number of UEs to more than 5, the data rate is reduced to less than 50 Mbps to keep the SINR at 13.6 dB or above for the OOK scheme. Based on the feedback signals from the PMU, the controller adjusts the data rate of each UE with the acceptable BER proposed for this system. Fig. 8 depicts the amount of electrical received power due to the CS at each UE that is served by Tx1. We consider five UEs that are distributed randomly in the coverage area of Tx1. Thus,

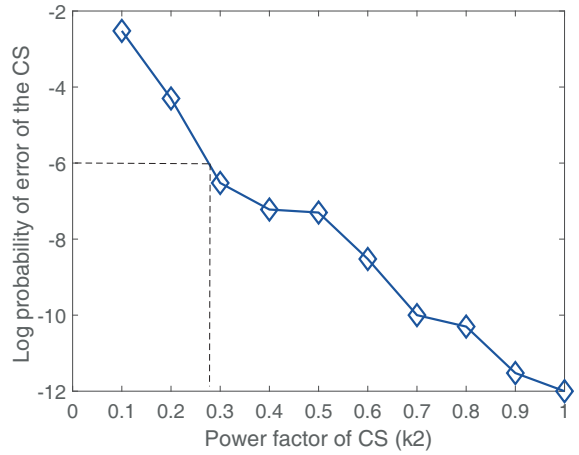

FIGURE 5. Log of the probability of error of the CS versus the power factor (k_2).

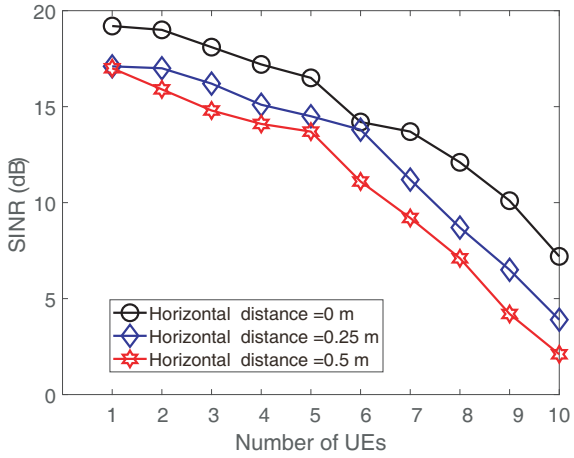

FIGURE 6. Effect of the number of UE on the SINR.

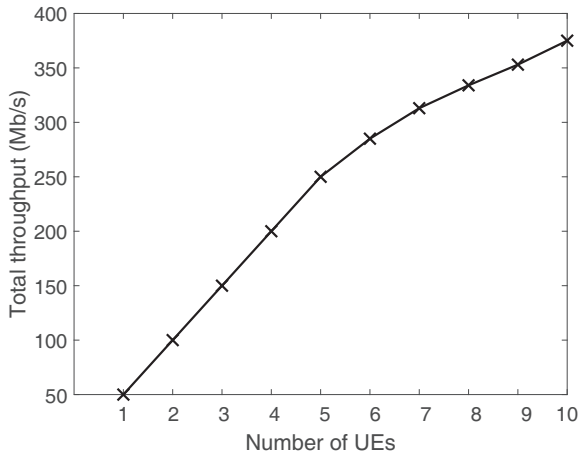

FIGURE 7. The total throughput of Tx1 versus the number of UEs.

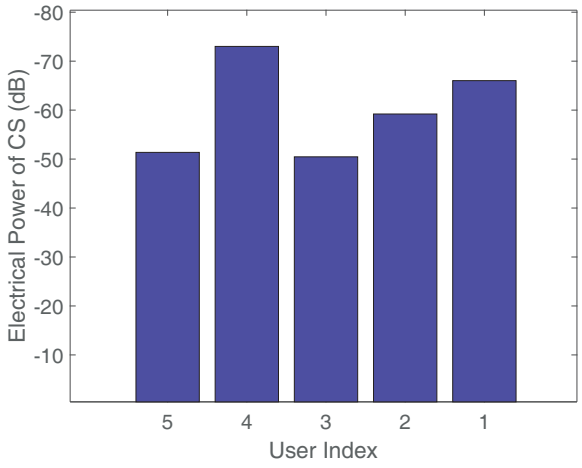

FIGURE 8. The electrical received power of the CS in the coverage area of Tx1.

each UE can be served with a data rate of 50 Mbps and BER not more than 10^{-6}. It should be noticed that in this work, we assume that there is no chance for any two UEs to be located at the same place, and the minimum distance between UEs is equal to 0.3 m. At each UE, the PMU calculates the electrical power of the CS that is related to Tx1 and informs the controller of the amount of electrical power of each UE. It is important to mention that Fig. 8 is obtained for one realization, i.e., the locations of all UEs are fixed during one run of the simulation.

4. CONCLUSIONS

In this paper, CSs are proposed for pairing algorithms, SIC, and load balancing for NOMA-VLC systems. The controller has been employed to manage the connection between Txs and UEs in this work. Each Tx has been given one unique CS, which was utilized to identify the Tx, find the associated UEs for each Tx, and measure the interference at each UE. Thus, each Tx sends two signals simultaneously, the data signal and the CS. At each UE, the PMU was used to calculate the power of each CS. Therefore, based on this measurement, the controller divided the UEs into small groups, and each group has been served by one Tx. Besides, each Tx divided its data signal between the associated UEs based on the feedback signal from the PMU. Moreover, the PMU informed the SIC block of the amount of interference that was evaluated by each UE. In this paper, each UE was served with a data rate of 50 Mbps and BER not more than 10^{-6} while the OOK scheme was utilized. Hence, the controller distributed the UEs based on this communication performance. The result showed that each Tx was able to serve up to 5 UEs with a data rate of 50 Mbps within the acceptable BER.

REFERENCES

[1] Yin, L., W. O. Popoola, X. Wu, and H. Haas, "Performance evaluation of non-orthogonal multiple access in visible light communication," *IEEE Transactions on Communications*, Vol. 64, No. 12, 5162–5175, 2016.

[2] Sünnetci, K. M. and M. Sönmez, "Variable pulse position modulation receivers for visible light communication systems without the knowledge of dimming level," *Transactions on Emerging Telecommunications Technologies*, Vol. 33, No. 5, e4445, 2022.

[3] Ali, Z., G. A. S. Sidhu, M. Waqas, and F. Gao, "On fair power optimization in nonorthogonal multiple access multiuser networks," *Transactions on Emerging Telecommunications Technologies*, Vol. 29, No. 12, e3540, 2018.

[4] Qian, J., L. Yu, C. Liu, X. Lv, Y. Wang, and Z. Wang, "Optimization design of RIS-assisted high-capacity visible light communications based on HDMA," *Physical Communication*, Vol. 58, 102056, 2023.

[5] Aljohani, M. K., O. Z. Aletri, K. D. Alazwary, M. O. I. Musa, T. E. H. El-Gorashi, M. T. Alresheedi, and J. M. H. Elmirghani, "Noma visible light communication system with angle diversity receivers," in *2020 22nd International Conference on Transparent Optical Networks (ICTON)*, 1–5, IEEE, 2020.

[6] Sadat, H., M. Abaza, S. M. Gasser, and H. ElBadawy, "Performance analysis of cooperative non-orthogonal multiple access in visible light communication," *Applied Sciences*, Vol. 9, No. 19, 4004, 2019.

[7] Kizilirmak, R. C., C. R. Rowell, and M. Uysal, "Non-orthogonal multiple access (NOMA) for indoor visible light communications," in *2015 4th International Workshop on Optical Wireless Communications (IWOW)*, 98–101, IEEE, 2015.

[8] Dogra, T. and M. R. Bharti, "User pairing and power allocation strategies for downlink NOMA-based VLC systems: An overview," *AEU — International Journal of Electronics and Communications*, Vol. 149, 154184, 2022.

[9] Younus, S. H., "Collaborative transmitters management for multi-user indoor VLC systems," *Transactions on Emerging Telecommunications Technologies*, Vol. 32, No. 10, e4319, 2021.

[10] Younus, S. H., "Interference mitigation in multiuser WDM VLC systems using differential receiver," *Transactions on Emerging Telecommunications Technologies*, Vol. 33, No. 9, e4512, 2022.

[11] Ho, K.-P. and J. M. Kahn, "Methods for crosstalk measurement and reduction in dense WDM systems," *Journal of Lightwave Technology*, Vol. 14, No. 6, 1127–1135, 1996.

[12] Chatterjee, S., D. Sabui, G. S. Khan, and B. Roy, "Signal to interference plus noise ratio improvement of a multi-cell indoor visible light communication system through optimal parameter selection complying lighting constraints," *Transactions on Emerging Telecommunications Technologies*, Vol. 32, No. 10, e4291, 2021.

[13] Gu, W., M. Aminikashani, P. Deng, and M. Kavehrad, "Impact of multipath reflections on the performance of indoor visible light positioning systems," *Journal of Lightwave Technology*, Vol. 34, No. 10, 2578–2587, 2016.

[14] Kahn, J. M. and J. R. Barry, "Wireless infrared communications," *Proceedings of the IEEE*, Vol. 85, No. 2, 265–298, 1997.

[15] Neumann, A., J. J. Wierer, W. Davis, Y. Ohno, S. R. J. Brueck, and J. Y. Tsao, "Four-color laser white illuminant demonstrating high color-rendering quality," *Optics Express*, Vol. 19, No. 104, A982–A990, 2011.

[16] Lee, K., H. Park, and J. R. Barry, "Indoor channel characteristics for visible light communications," *IEEE Communications Letters*, Vol. 15, No. 2, 217–219, 2011.

[17] Chun, H., S. Rajbhandari, G. Faulkner, D. Tsonev, E. Xie, J. J. D. McKendry, E. Gu, M. D. Dawson, D. C. O'Brien, and H. Haas, "Led based wavelength division multiplexed 10 Gb/s visible light communications," *Journal of Lightwave Technology*, Vol. 34, No. 13, 3047–3052, 2016.

[18] Younus, S. H., A. A. Al-Hameed, A. T. Hussein, M. T. Alresheedi, and J. M. H. Elmirghani, "Parallel data transmission in indoor visible light communication systems," *IEEE Access*, Vol. 7, 1126–1138, 2018.

[19] Leskovar, B., "Optical receivers for wide band data transmission systems," *IEEE Transactions on Nuclear Science*, Vol. 36, No. 1, 787–793, 1989.

[20] Gfeller, F. and U. Bapst, "Wireless in-house data communication via diffuse infrared radiation, RZ 941 (32513)," *Information Systems*, Vol. 5, No. 3, 248, 1980.

[21] Almohimmah, E. M., M. T. Alresheedi, A. F. Abas, and J. Elmirghani, "A simple user grouping and pairing scheme for non-orthogonal multiple access in VLC system," in *2018 20th International Conference on Transparent Optical Networks (ICTON)*, 1–4, IEEE, 2018.

[22] Al-Hameed, A. A., S. H. Younus, A. T. Hussein, M. T. Alresheed, and J. M. H. Elmirghani, "LiDAL: Light detection and localization," *IEEE Access*, Vol. 7, 85 645–85 687, 2019.